Detecting subsurface groundwater flow in fractured rock using self-potential (SP) methods

Fritjof Fagerlund · Graham Heinson

Abstract In the wine district of Clare Valley in South Australia, the natural-voltage SP signal generated by fluid flow in fractured rock during a pumping test was carefully monitored by time-continuous measurements. From ten electrode locations surrounding the pumping well, the drawdown cone produced by pumping was determined on the basis of the SP measurements together with laboratory measurements of the grain-boundary ζ (zeta)-potential. Such measurements allowed calculation of the fractured-rock aquifer's transmissivity and average permeability. Results were confirmed by piezometer measurements to the extent that data were available. The study has revealed that SP signals generated during pumping tests are of a complex nature. However, if the pumping test is sufficiently long to allow the signal to stabilise, and careful field procedures are in place, then SP measurements have the potential to add significant hydrogeological information. SP measurements are relatively easy and cheap, and are, contrary to traditional methods, not restricted to the locations of existing piezometers, which is particularly useful in fractured-rock aquifers.

Introduction

As it becomes more important to manage and preserve our fresh-water resources, there is also an increasing need for new and efficient methods of hydrogeological investigation. Electrical methods have been used to monitor groundwater occurrence within fractured rock with some success. Such measurements provide information on the fluid electrical conductivity and the fractured rock porosity. However, determining permeability is more difficult, and the primary technique involves pumping tests monitored at adjacent boreholes. Although such measurements provide excellent point calibrations of fluid flow, fractured rock systems are heterogeneous, and it may not be possible to extrapolate single measurements to a greater volume.

An alternative is to measure the electric potential occurring naturally on the ground surface, the self-potential (SP) (sometimes also called natural potential, NP). Its main sources are electrokinetic potentials produced by fluid and heat fluxes in the ground, diffusion potentials across boundaries between regions of different chemical composition and redox reactions around orebodies and buried metallic objects. In particular, the streaming of water through pores and fractures in the ground produces an electric potential gradient, called streaming potential, along the flow path. Hence, unlike for other geophysical methods, there is a direct link between SP and groundwater flow.

Traditionally, SP surveys mainly involved the measuring of diffusion potentials in well logging for oil prospecting, and redox-related potentials generated by orebodies in base metal prospecting. Recently, streaming potentials have become more important due to applications in geothermal prospecting (Corwin and Hoover 1979; Ishido and others 1983; Sill 1983; Morgan and others 1989; Ishido and Pritchett 1999; Revil and others 1999b) and earthquake prediction (Ishido and Mitzutani 1981; Jouniaux and Pozzi 1995b). In hydrogeological investigations, streaming potential measurements have among other things been used to study groundwater movements and flow paths (Schiavone and Quarto 1984; Fournier 1989), to map sinkholes in a karst area (Wanfang and others 1999) and to monitor fluid flow in the sediments of a subduction zone subjected to compression (Heinson and Segawa 1997).

Streaming potentials generated by leakage from a reservoir and water flow towards a well during pumping have been studied by Bogoslovsky and Ogilvy (1972), Parasnis (1986) and Ogilvy and others (1989). These studies show that under favourable conditions, the SP anomaly around a

Received: 5 November 2001 / Accepted: 27 August 2002
Published online: 22 October 2002

F. Fagerlund (✉)
Department of Earth Sciences, Hydrology,
Uppsala University, Geocentrum, Villavägen 16,
SE-752 36 Uppsala, Sweden
E-mail: fritjof.fagerlund@hyd.uu.se
Tel.: +46-18-4712259
Fax: +46-18-551124

F. Fagerlund · G. Heinson
Department of Geology and Geophysics,
University of Adelaide, Adelaide,
South Australia 5005, Australia

 DOI 10.1007/s00254-002-0693-x

pumping well is a mirror image of the drawdown cone, and, accordingly, Bogoslovsky and Ogilvy (1972) suggest that SP measurements are better than a sparse network of piezometers for measuring the drawdown. However, few similar studies have been carried out, and SP surveys described by Jansen and Zorich (1995) do not show an equally straightforward relationship between measured SP and drawdown.

Indeed, SP methods are not widely used in this context due to signal noise and ambiguity of interpretation, the main problems being (1) to isolate the signal from electrode drift and background noise (other SP sources) and (2) to correctly interpret the SP signal at the ground surface in order to determine the sub-surface fluid flow. However, if these problems are overcome SP measurements have the potential to greatly facilitate pumping tests, especially in anisotropic aquifers. Without the restriction to measurements at the locations of piezometers it would be possible to determine the drawdown cone, along with permeability and preferred flow paths, with far greater accuracy. Furthermore, SP is cheap to use and provides a volumetric average, rather than a point measurement, of the fluid flow properties in the region of interest.

The objective of this study was to evaluate and develop the SP method in conjunction with pumping tests in fractured rock aquifers, using three approaches:

1. Using measurements of electrokinetic potentials during pumping tests to determine sub-surface fluid-fluxes and hence obtain permeability and heterogeneity;
2. Developing modelling techniques to interpret SP signals from pumping tests;
3. Building a laboratory experiment setup to measure the streaming potential for given rock types and fluids relevant to the study, thus providing a means to quantify SP data and a comparison with results from the field.

Clare Valley

Fractured rock aquifers underlie approximately 40% of the Australian continent and are becoming increasingly important as water supplies, as the better-known porous aquifers are almost fully utilised (Love and Cook 1999). Because they are often highly heterogeneous and anisotropic, studies of these groundwater systems can be tedious and there is a need for easy methods of investigation. Some examples of problems that pose a challenge in the fractured rock environment are well siting for maximum yield and avoidance of well interference, mapping of contaminant migration and determination of sustainable yields.

The Clare Valley is situated in the Northern Mount Lofty Ranges, approximately 100 km north of Adelaide, South Australia (Fig. 1). The area is well known for its high-quality wines, and as the viticultural industry is expanding there is an increasing demand for water. Approximately 60% of the water used for irrigation (1,400 ML/annum) is sourced from groundwater (Morton and others 1998). To ensure sustainable development and avoid exhaustion of

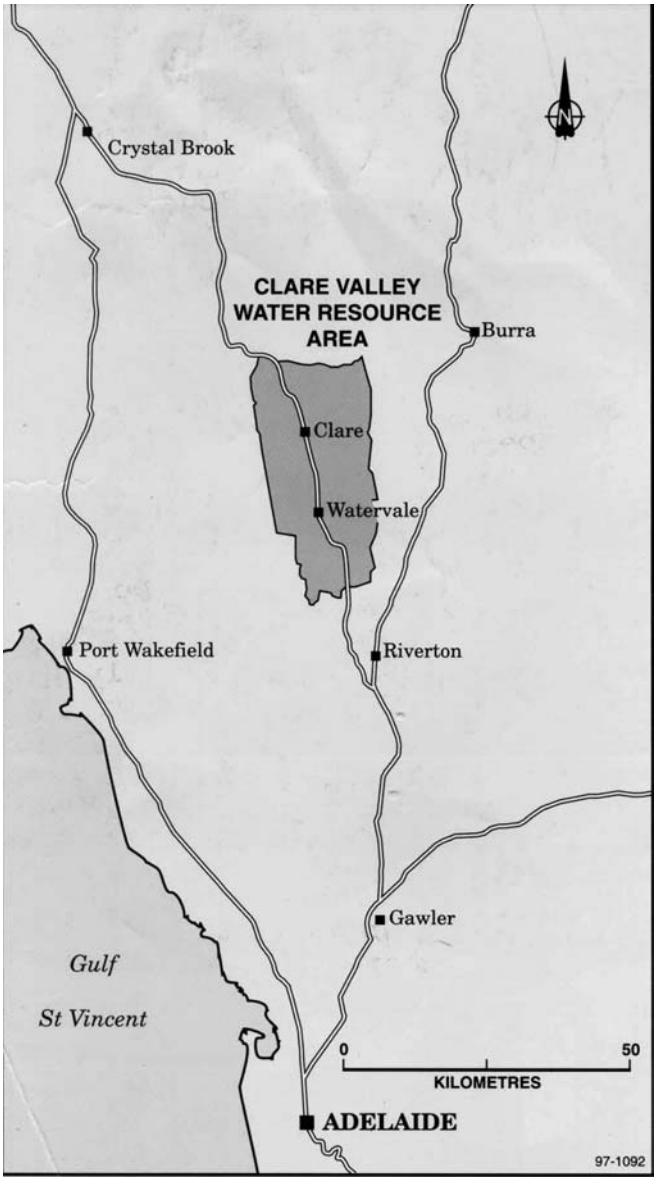

Fig. 1
Clare Valley water resource area. (Adapted from Love and Cook 1998)

fresh-water resources, good management and understanding of the groundwater system is needed. Consequently, studies have been undertaken in several test areas with a number of boreholes drilled for testing.

Clare Valley is a syncline with its fold axis in the north–south direction. The western limb of the fold is overturned with bedding planes dipping more than 90° whereas the eastern side is dipping more mildly (Winsor 1995). The groundwater is stored in Proterozoic rocks of the Adelaide Geosyncline. The dominant lithologies are siltstones, shales, dolomites and quartzites (Morton and others 1998), which are common to many similar systems in Australia. The groundwater availability appears to be controlled by closely spaced (<20 m), small-aperture fractures, which have no obvious surface expression (Love and Cook 1999). Yield, permeability and salinity vary considerably over short distances. Well yields vary between less than 0.1 to

25 L/s and salinity between less than 500 to in excess of 7,000 mg/L (Morton and others 1998).
A pumping test was scheduled by the Department for Water Resources South Australia at Watervale Oval on the western side of the syncline (see Fig. 1) at a suitable time for the study and this site was hence chosen for taking SP measurements during pumping.

Theory

The streaming potential

Streaming potentials or electrokinetic potentials are caused by the motion of ions with the flow of a liquid. In a system consisting of two separate phases such as liquid and a solid medium, there has to be a total balance of charge, that is, the system has to be electroneutral. This means that the net charge within the liquid and the charge on the surface of the solid medium have to be equal in magnitude and of opposite signs. At the interface of the two phases there is an aggregation of excess charge (excess ions and/or electrons) on each side, which constitutes an electrical double layer. The electrical double layer, which is crucial for the generation of streaming potentials, can be described by models of various complexities.
In the Gouy-Chapman (one-layer) model the electrical double layer is described as a uniform surface charge on the solid medium, which is balanced by a surplus of ions of opposite sign (positive ions if the surface is negatively charged) in the liquid phase, forming a diffuse layer where the charge density, q, is greatest nearest the solid wall and then decreases, in accordance with a Boltzmann distribution of the ions, to approach zero at some distance (Overbeek 1952; Morgan and others 1989). According to the Stern model, which is a further development of the Gouy-Chapman model, there is a layer of more strongly adsorbed ions, called a Stern (or Helmholz) layer, next to the solid surface, followed by a diffuse layer as described above (Fig. 2). Normally, for rock–water systems, the surface charge is negative, and hence the electric potential V is lowest at the solid surface. It increases linearly in the Stern layer and then approaches zero as the remaining charge offset is balanced out by ions in the diffuse layer. Note that if the adsorption of ions is very strong in the Stern layer the potential may rise above zero and will then decrease as it approaches zero in the diffuse layer (Fig. 2b). The plane closest to the solid surface in which movement can take place is called the hydrodynamic slipping plane S. The slipping plane constitutes the boundary between the mobile phase (fluid) and the immobile phase (solid medium plus immobile fluid) and is usually close to the plane H separating the Stern and diffuse layers (Fig. 2). When the fluid moves relative to the solid medium, the mobile part of the electrical double layer is dragged along with the flow. Hence there is a transport of electric charge with the flow, which constitutes a convective (or drag) electric current. The amount of charge transported is directly related to the potential on the slipping plane, the ζ-potential (zeta-potential), the magnitude of which equals the potential change in the mobile phase. The more negative the ζ-potential the more positive ions are transported with the flow, and the more positive it is the greater is the net transport of negative charge (ions). For a zero ζ-potential no convective current or corresponding streaming potential gradient are produced.
Assuming that (1) the flow is laminar and (2) the radius of curvature of the capillary or pore is much bigger than the thickness of the double layer, the convective electric current per unit area, i_{conv}, over a capillary or pore is given by:

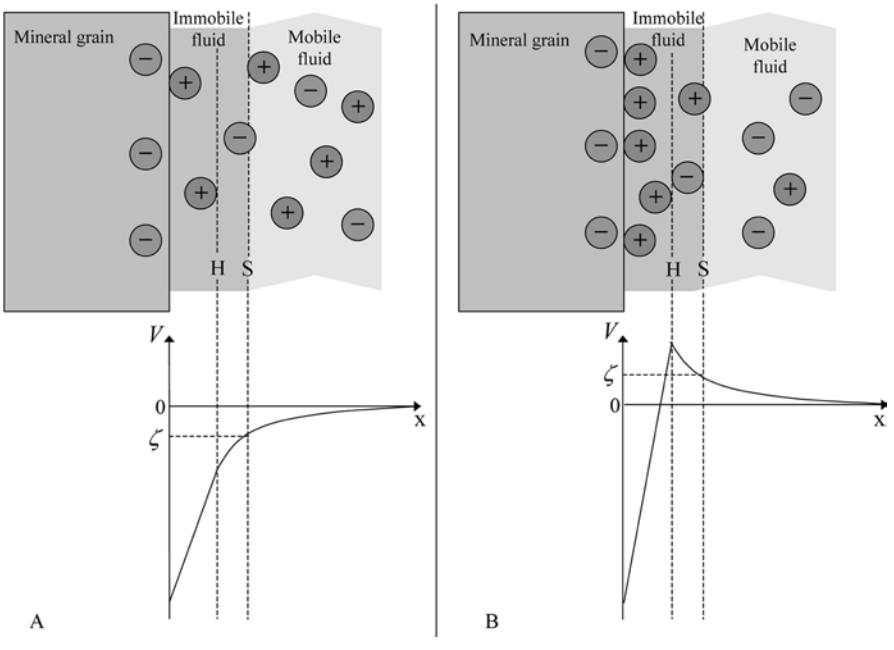

Fig. 2
The electrical double layer at a rock–water interface according to the Stern model. *Below* The electric potential (V) as a function of distance (x) from the pore wall. The hydrodynamic slipping plane (S) separates the mobile and immobile phases of the fluid. The potential at this plane is called the zeta-potential (ζ). Depending on amount of specific adsorption in the Stern layer between the pore wall and plane H, ζ can be positive (**b**) or negative (**a**). For a negative ζ, more positive than negative ions are transported with the fluid

$$i_{conv} = \frac{\zeta \varepsilon_r \varepsilon_0}{\eta} \overline{\nabla_n P} \quad (1)$$

where ζ is the ζ-potential, ϵ_r is the relative dielectric constant of the liquid and ϵ_0 is the dielectric constant of vacuum, η is the viscosity of the fluid and $\overline{\nabla_n P}$ is the mean pressure gradient normal to the cross-section area. A derivation of Eq. (1) is given in Overbeek (1952). Note that since the fluid flows in the direction of negative pressure gradient ($-\nabla P$), and as ϵ_r, ϵ_0 and η are positive constants, if ζ is negative, i_{conv} is positive in the direction of flow, and there is a transport of positive charge (ions) with the flow. As a consequence of the convection current, an electric potential gradient (streaming potential) generates along the flow path. The potential gradient causes current to flow back through the liquid by conduction. The conduction current per unit area, i_{cond}, over a cross section is given by Ohm's law:

$$i_{cond} = -\sigma \overline{\nabla_n V} \quad (2)$$

where σ is the bulk conductivity of the liquid and $\nabla_n V$ the potential gradient normal to the cross section. In the absence of other (external) current sources the total current is the sum of the convective and conductive currents, $i_{total}=i_{conv}+i_{cond}$. For steady-state conditions the convective current produced by fluid flow is completely balanced by the return conduction current $i_{cond}=-i_{conv}$ and the total current equals zero. Now combining Eqs. (1) and (2) results in a directly proportional relationship between $\nabla_n V$ and $\nabla_n P$ known as the Helmholz-Smoluchovsky equation:

$$\overline{\nabla_n V} = \frac{\varepsilon_r \varepsilon_0 \zeta}{\eta \sigma} \overline{\nabla_n P} = C_s \overline{\nabla_n P} \quad (3)$$

where $C_s=\epsilon_r\epsilon_0\zeta/\eta\sigma$ is the streaming potential coefficient. The conductive part of the current flow can, however, only be described by Eq. (2) provided that conduction takes place solely in the bulk fluid. If conduction on the mineral grain surfaces is significant, which is often the case for low-concentration electrolytes (low bulk fluid conductivity), then the return current flows both in the fluid and on the surface of the surrounding medium. Accounting for surface conductance, Eq. (3) transforms to:

$$\frac{\overline{\nabla_n V}}{\overline{\nabla_n P}} = \frac{\varepsilon_r \varepsilon_0 \zeta}{\eta\left(\sigma + 2\sigma_s/r\right)} \quad (4)$$

for a cylindrical pore of radius r and where σ_s is the specific surface conductance (Overbeek 1952).
Groundwater flow is, however, driven by the hydraulic head gradient, ∇H, rather than ∇P. Since $P=\rho g H$, where ρ is the density of the fluid (in kg/m^3), g is the specific gravity (9.81 m/s^2) and H the hydraulic head, Eq. (3) can be written as:

$$\overline{\nabla_n V} = \frac{\varepsilon_r \varepsilon_0 \zeta \rho g}{\eta \sigma} \overline{\nabla_n H} = C_s' \overline{\nabla_n H} \quad (5)$$

It can be concluded that the streaming potential gradient is proportional to the pressure gradient, and in the controlled environment of the laboratory Eqs. (3) or (5) are excellent for determining C_s and ζ. Several studies have been carried out to determine the ζ-potential for different types of rock, as well as to investigate the dependency of C_s and ζ on various environmental parameters such as pH, temperature, grain size, permeability, electrolyte concentration and valency (for example, Ahmad 1964; Ishido and Mizutani 1981; Morgan and others 1989; Jouniaux and Pozzi 1995a, 1995b; Truesdail and others 1998; Lorne and others 1999; Revil and others 1999a, 1999b).

Groundwater flow towards a production well

In models relating streaming potentials to groundwater flow, the groundwater flow can be regarded as the primary flow producing the secondary electric current flow. In principle, the two flows are interdependent and are referred to as coupled. The effect of current flow on groundwater flow (electro-osmosis) can, however, safely be neglected for normal rock–water systems (see Sill 1983; Fitterman 1978; Ishido and Pritchett 1999). The groundwater flow can normally be described by Darcy's law:

$$\frac{Q}{A} = -\frac{k}{\eta}\nabla P = -\frac{kg\rho}{\eta}\nabla H = -K\nabla H \quad (6)$$

where Q is the fluid flux (volume/time), A the cross-sectional area, k the intrinsic permeability (in m^2) and K the hydraulic conductivity (in m/s). $Q/A=v$ is the Darcy-velocity in m/s.
A relatively simple model of the groundwater flow towards a production well can be obtained by assuming the following:

1. Darcy's law holds.
2. The aquifer is homogenous, isotropic and of infinite areal extent.
3. The piezometric surface before pumping is horizontal.
4. The well fully penetrates the aquifer, which is bounded by a horizontal confining bottom.
5. Water is instantaneously removed from storage upon a decline in head.
6. Steady-state conditions have been reached, that is, drawdown does not change with time.

Under these assumptions the groundwater flow towards a production well in an unconfined aquifer can be described by Thiem's equation (Bear 1979; Fetter 1994), which is given by:

$$H_2^2 - H_1^2 = \frac{Q}{\pi K}\ln\left(\frac{r_2}{r_1}\right) \quad (7)$$

where H_1 and H_2 are the heads at radial distances r_1 and r_2 from the production well respectively. Note that the drawdown $d=H_0-H$, where H_0 is the head before pumping, and that the hydraulic head is equal to the saturated thickness of the aquifer.
Fractured rock aquifers are usually complicated systems. Whether the fractured rock aquifers of Clare Valley should be regarded as confined or unconfined is not obvious and may be different from site to site. A system of mainly horizontally orientated fractured planes

occurring at some depth would be more similar to a confined than an unconfined porous aquifer. If the fractures are mainly vertical and the fracture connectivity is good, the system would show unconfined characteristics. However, for low drawdowns compared to the original saturated thickness H_0, the difference between confined and unconfined aquifers becomes very small (Bear 1979). It is clear that most of the assumptions underlying Eq. (7) will not be completely satisfied in fractured rock systems, which are likely to show at least some anisotropy and heterogeneity. Anisotropy can be estimated by applying the above theory to drawdown data collected in different directions from the pumping well and calculating the (apparent) hydraulic conductivity in each direction. The quotient K_{max}/K_{min} gives some information about the anisotropy.

Methods and results

General methodology

The general approach of this study follows a methodology in five steps:

1. Field measurements: the spatial SP distribution and the change in SP with time are measured during pumping tests.
2. Laboratory measurements: the ζ-potentials of the rock types of interest are determined in the laboratory.
3. SP modelling and interpretation: the SP signal is analysed in order to find a spatial pressure distribution (drawdown) that would produce the measured SP at ground surface.
4. Groundwater flow model: when spatial drawdown due to pumping has been determined, these data are interpreted in a hydrogeological context and a model of the groundwater flow is constructed. Permeability and anisotropy are calculated.
5. Validation: to validate the efficiency of the method the results are compared to drawdown measured in existing observation wells at the test sites. Laboratory and field results are also compared.

Three parameters are needed as input for the SP modelling. Firstly, the spatial SP distribution is measured in the field. Secondly, the streaming-potential coefficient C_s, relating potential to pressure, is determined from the ζ-potential, measured in the laboratory. Thirdly, information (or assumptions) about the resistivity of both the fluid and surrounding medium are needed to model the total current flow and relate surface SP to sub-surface current sources (fluid flow). For a general situation with no pumping, the output would be the potentiometric surface. When taking SP measurements during a pumping test the output is the spatial drawdown or change in potentiometric surface. The thus obtained drawdown data are used as input for the groundwater model from which permeability and anisotropy can be calculated and the general flow pattern and preferred flow paths can be analysed.

Laboratory work

Apparatus

To relate the streaming potential V measured in the field to the drawdown, an apparatus to determine the streaming-potential coefficients C_s and the ζ-potentials of given rock types and electrolytes was built, as shown in Fig. 3. The apparatus consists of a tank connected to a plastic tube containing a crushed sample of the rock type of interest. The tube is a screw-in piece and can therefore easily be changed. It has an inner diameter of 1.8 cm and the length inside the stopper pieces, l, is 29 cm. At each end of the sample tube there is a stopper made of several layers of plastic netting (fly net), forming a mesh fine enough to keep the crushed rock sample in place while water flow through it is still permitted. The tube is connected to an inflow and outflow chamber at each end. In each chamber there is a manometer, a transparent narrow plastic tube in which fluid can rise vertically, thus allowing the hydraulic head at each end to be measured. Additionally, there is an Ag-AgCl electrode in each chamber, which allows measurements of the electric potential difference (the streaming potential) over the tube. The tank connected to the inflow chamber can be placed at different heights so that different head gradients ∇H (or pressure gradients ∇P) driving the flow through the tube are produced. The tank has a relatively large base area (roughly 600 cm^2), which ensures that for slow flows ∇H does not change significantly with time unless the tank is moved vertically.

Crushed rock samples and electrolytes

To represent the fractured rock aquifers of Clare Valley three samples were collected from two quarries in the vicinity of the test area. Two samples (Q1A and Q1B) were

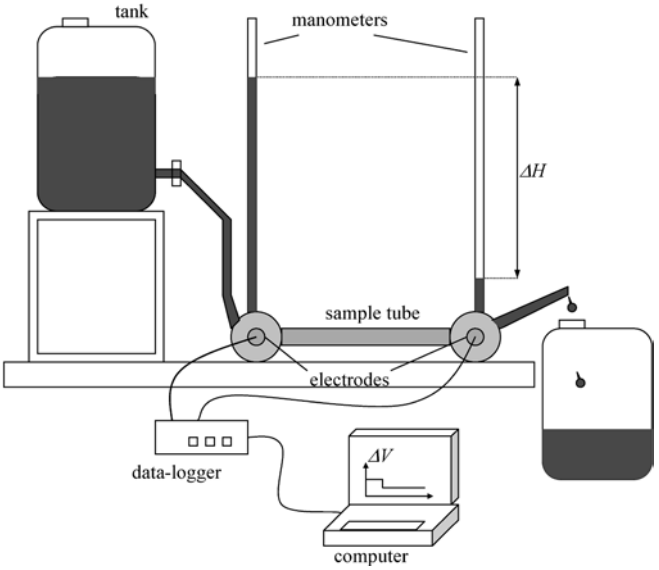

Fig. 3
Streaming-potential measurement apparatus

collected from the first quarry, and one (Q2) from the second quarry. The rocks are similar, but there are some differences in clay- and quartz-content and degree of metamorphism. Q1A is a soft shale with higher clay content than the other samples. Q1B can be classified as a fine sandstone or siltstone. It is the hardest of the samples and consists mainly of quartz. Q2 consists of layers of shale and siltstone and can be seen as an intermediate between Q1A and Q1B.

The rocks were crushed with a jaw-crusher and then sieved with a combination of sieves (850-, 500-, 250- and 100-μm mesh size), giving samples of different grain size for each rock type. Each sample was then carefully washed to remove all dust-like, fine particles adsorbed on the surfaces of the grains. After washing, the sample was tightly packed into a sample tube and the stoppers put in place at each end. The fluid used was distilled water with added pure sea salt to produce the conductivity wanted. For the Clare Valley rocks two electrolytes were used, one was fresh water with very low salinity (σ=70 μS/cm) and one had a salinity typical of the slightly saline aquifers (σ=1,470 μS/cm).

ζ-potential measurements

Potential difference V between the two electrodes was measured with a model D50 Data-Taker data-logger ($V=V_{outlet}-V_{inlet}$) and logged on a laptop computer every 5 or 10 s. The pressure driving the flow is measured as hydraulic head difference H in centimeters of water, over the sample tube, which is given by $H=H_{outlet}-H_{inlet}$ (measured in the direction of flow). The reference (datum) is hence the water level of the inflow manometer and H is negative. Since both the potential and hydraulic gradients are uniform over the sample tube, Eq. (5) simplifies to $V=C_s'H+V_{offset}$, where V_{offset} is the offset between the two electrodes.

The offset in potential (V_{offset}) is a constant, provided that there is no electrode drift. While V was logged continuously, the tank was moved up or down stepwise, producing different H. By measuring V for different H, C_s' (and V_{offset}) can be determined by linear regression and ζ is then calculated from $C_s'=\epsilon_r\epsilon_0\zeta\rho g/\eta\sigma$. The fluid electrical conductivity σ and the temperature T were measured with a TPS-84 salinity/conductivity meter in both the inflow and outflow tanks. Values of ϵ_r and η for water can be calculated from the temperature: $\epsilon_r=88.15-41.4\times(T/100)+13.1\times(T/100)^2-4.6\times(T/100)^3$ (Kaye and Laby 1986), where T is the temperature in degrees Centigrade. Based on data from Kaye and Laby (1986), a linear approximation $\eta(T)=0.0272T+1.546$ which gives η in milliPascal-seconds (mPa-s) has been used for temperatures between 15 and 20 °C. Free space dielectric permittivity $\epsilon_0=8.85\times10^{-12}$ F/m and it was assumed that ρ=1,000 kg/m^3 and g=9.81 m/s^2. Normally, it took some time for a fresh combination of rock sample and fluid to obtain a stable streaming potential and a negative peak was observed when the inflow tank was opened and flow through the sample began (for the first time, or after a period of no flow with the sample saturated inside the tube). Therefore, the fluid was allowed to flow through the sample until the potential remained constant for a constant pressure gradient. A close-up of the experiment part when H is varied stepwise is shown in Fig. 4. The potential difference V increases with increased flow through the sample. A linear regression of the values of V and H for each step in Fig. 4 is shown in Fig. 5, which enables C_s' and V_{offset} to be determined. According to Fig. 5, the streaming potential coefficient C_s'=–0.018 and the constant offset between the electrodes V_{offset}=–5.324 mV. The ζ-potential for the sample is now easily calculated as described above. A summary of the results is presented in Table 1.

For the experiments with low fluid electrical conductivity (σ ≈70 μS/cm), the ζ-potentials calculated under the assumption that there is no surface conductance are probably incorrect, since for such low σ values surface conductance is in fact very likely to be significant. The ζ-potentials calculated from the experiments with higher fluid electrical conductivity (σ ≈1,470 μS/cm) and low permeability are much more consistent for the different series and are reasonable in comparison with data presented by Truesdail and others (1998) and Lorne and others (1999). Hence, the results of the ζ-potential measurements of samples from the Clare Valley can be summarised as follows:

Q1A (soft shale with clay)ζ=–15±2 mV
Q1B (fine sandstone)ζ=–40±1 mV
Q2 (layers of shale and siltstone)ζ=–23±1 mV

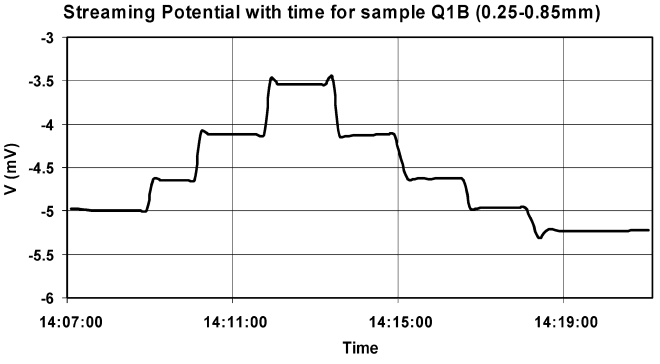

Fig. 4
Close-up of a typical streaming-potential experiment in the laboratory. As H is varied in steps, V responds proportionally

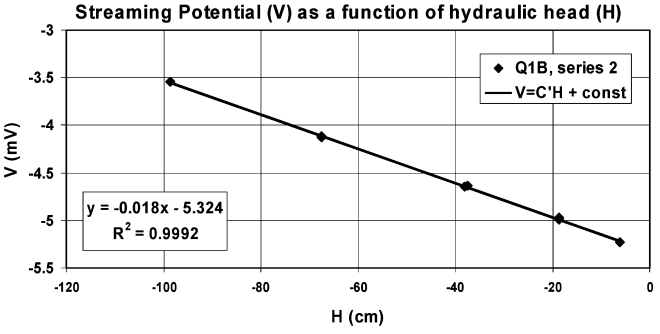

Fig. 5
Linear regression of values of V and H producing the relationship $V=C_s'H+V_{offset}$. For this sample and electrolyte, regression gives C_s'=–0.018 mV/cm and V_{offset}=–5.324 mV

Table 1
Summary of laboratory measurements. *Cond.* Electric conductivity; *K* hydraulic conductivity; *Temp.* temperature; C_s streaming-potential coefficient; *Visc.* viscosity; ϵ_0 dielectric constant of vacuum; ϵ_r relative dielectric contant; *Zeta-pot.* zeta-potential

Sample	Grain size (mm)	Series	Cond. (mS/cm)	K (cm/s)	Temp. (°C)	C'_s (mV/cm)	C_s (mV/Pa)	Visc. (mPa-s)	$\epsilon_0\epsilon_r$ (F/m)	Zeta-pot. (mV)
Q1A: soft shale with some clay	0.5–0.85	1	0.0705	0.110	18.4	−0.0885	−9.0E-04	1.046	7.16E-10	−9.3
		2	0.0705	0.110	18.4	−0.0971	−9.9E-04	1.046	7.16E-10	−10.2
		3	0.0705	0.110	18.4	−0.0655	−6.7E-04	1.046	7.16E-10	−6.9
		Average	0.0705			−0.0837				−8.8
	0.25–0.5	1	0.07	0.040[a]	17	−0.0544	−5.6E-04	1.084	7.21E-10	−5.8
		2	0.071	0.040[a]	18	−0.0771	−7.9E-04	1.056	7.18E-10	−8.2
		3	0.071	0.040[a]	17.7	−0.0824	−8.4E-04	1.065	7.19E-10	−8.8
		4	0.075	0.040[a]	17	−0.1226	−1.3E-03	1.084	7.21E-10	−14.1
		5	0.075	0.040[a]	17	−0.1198	−1.2E-03	1.084	7.21E-10	−13.8
		Average	0.0724			−0.0913				−10.2
	0.5–0.85	1	1.469	0.070	17.5	−0.0073	−7.4E-05	1.070	7.19E-10	−16.3
		2	1.469	0.070	17.5	−0.0060	−6.1E-05	1.070	7.19E-10	−13.4
		Average	1.469			−0.0067				−14.8
Q1B: fine sandstone	0.25–0.85	1	1.468	0.060	17.8	−0.0180	−1.8E-04	1.062	7.18E-10	−39.9
		2	1.468	0.060	17.8	−0.0179	−1.8E-04	1.062	7.18E-10	−39.6
		Average	1.468			−0.0180				−39.7
Q2: layers of shale and siltstone	0.5–0.85	1	0.072	0.180	18.2	−0.0322	−3.3E-04	1.051	7.17E-10	−3.5
		2	0.072	0.180	17.5	−0.0348	−3.6E-04	1.070	7.19E-10	−3.8
		3	0.072	0.229	18	−0.0609	−6.2E-04	1.056	7.18E-10	−6.6
		Average	0.072			−0.0426				−4.6
	0.25–0.85	1	1.469	0.018	17.1	−0.0102	−1.0E-04	1.081	7.21E-10	−22.9
		2	1.469	0.018	17.1	−0.0101	−1.0E-04	1.081	7.21E-10	−22.7
		Average	1.469			−0.0102				−22.8
Beach sand	0.1–0.7	1	66	0.015	18.2	−0.0008	−8.2E-06	1.051	7.17E-10	−79.0

[a]Approximately

This shows that there are large differences in ζ-potential over short distances. The samples Q1A and Q1B were collected at the same quarry and were only separated by a few metres. The results indicate that the magnitude of the ζ-potential may be negatively related to clay content and positively related to the quartz content of the rock. Of the Clare Valley samples, Q1A had the highest clay content and lowest quartz content whereas Q1B had the highest quartz content and very little clay. The beach sand was nearly pure quartz and also had the highest ζ-potential, ζ=–80±10 mV. As a comparison, Lorne and others (1999) give ζ=–40±5 mV for Fontainebleau sandstone (99% quartz) and ζ=–12±0.2 mV for Houiller sandstone (quartz with anthracite and clay beds). Truesdail and others (1998) report ζ=–68±3 mV for Ottawa sand and ζ=–96±3 mV for pure silica. The ζ-potentials determined in this study are hence similar to results in previous studies for similar rocks. Due to the high salinity of the electrolyte used with the beach sand, the signal was very low and the error margin is hence large. It was, however, shown that even at these salinities, streaming-potentials are measurable.

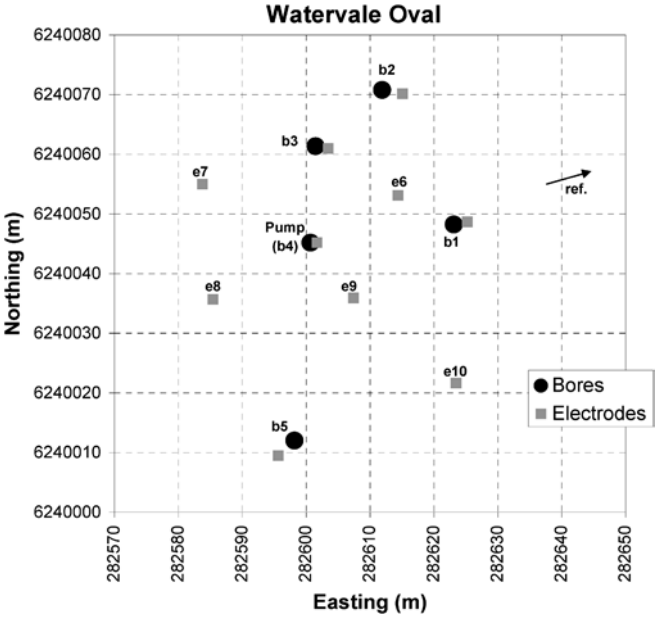

Fig. 6
Map showing boreholes and electrodes at Watervale Oval

Field survey at Watervale Oval

SP and drawdown measurements

Ten porous-pot Cu-$CuSO_4$ electrodes were placed around the pumping well at the test site at Watervale Oval as shown in Fig. 6. A reference electrode was placed approximately 200 m east-northeast of the pumping well and was relatively unaffected by the pumping. SP was measured as the difference in electric potential between the reference electrode and all other electrodes. A measurement was taken every 15 s with two model D-50 Data-Takers (a five-channel data logger with internal memory) and either directly logged onto a laptop computer or stored in the Data-Taker's internal memory. An electrode was placed near each borehole to allow for comparison between drawdown in the well and SP measured with the electrode. The electrodes were named b1–b5 (b for bore) and e6–e10 (e for extra). An average of

every four measurements was calculated to produce a value every minute, which improves signal-to-noise ratios. The pumping test started at 10:05 a.m. and finished at 6:05 p.m. on 9 April 2001. Borehole 4 was the pumping well and the rate of pumping was 2 L/s for the first 100 min and 1.5 L/s for the rest. The fluid electrical conductivity, temperature and pH were measured continuously in the pumping well. Drawdown was measured continuously in all wells. At the end of the pumping test the potentiometric surface had stabilised in the wells, which can be seen in Fig. 7, showing drawdown as a function of time.

SP was recorded during the whole period of pumping plus a short time before and after. SP as a function of time at three of ten electrodes is shown in Fig. 8. The SP signals recorded by the other seven electrodes were similar in shape but showed different start and end values.

From the time-continuous SP measurements (Fig. 8), a number of observations can be made. The SP signals at the different electrode locations are all unique but show many similarities. The high peak in the signal after about 20 min of pumping is caused by watering of the reference electrode. There is an increasing and then decreasing trend at all electrodes from about time=50 to 450 min. There is more noise in the data recorded by Data-Taker 1 (electrodes b1–b5). Some smaller peaks can be seen in all the signals, the most prominent being the one between approximately 420 and 430 min. At the end of pumping (480 min) all electrodes showed a higher SP value compared to before pumping started. The values before and at the end of pumping are especially useful in the further analysis and are indicated in Fig. 8. Care has to be taken when determining the "before" (or "start") value since there are some negative peaks due to electrode watering just before the pumping started, which can be seen in electrodes e6 and e10 (and b2 and e7, not showed here).

Model

From the Helmholz-Smoluchovsky equation [Eqs. (3), (4) or (5)], it can be seen that for the normal case when $\zeta < 0$ and hence also $C_s < 0$, the potential V increases ($\nabla V > 0$) with decreasing pressure ($\nabla P < 0$). As a consequence, in areas of groundwater recharge (infiltration) negative SP anomalies will be found, and in areas of discharge (such as

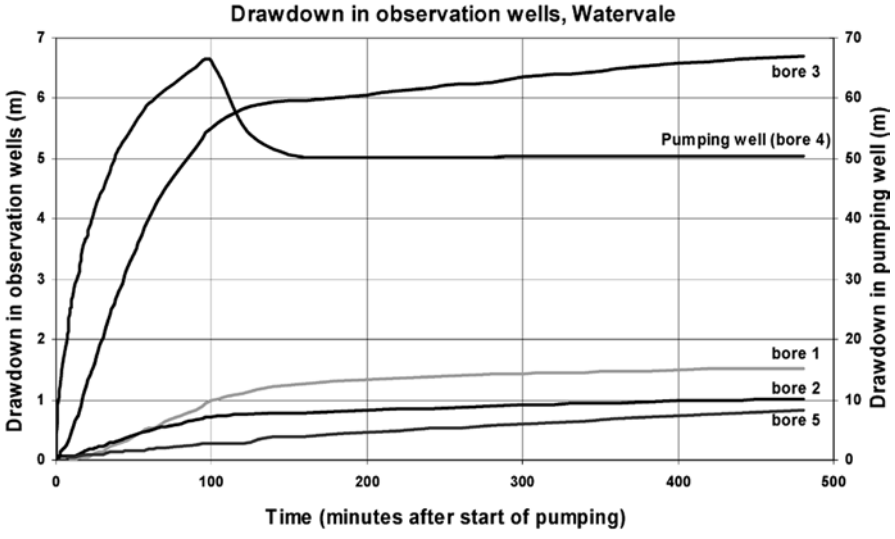

Fig. 7
Drawdown in the pumping and observation wells as a function of time

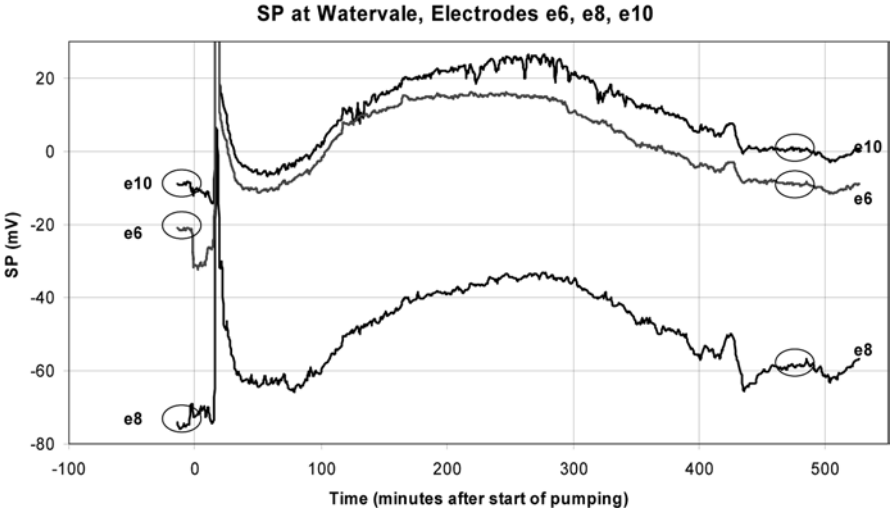

Fig. 8
SP with time at electrodes e6, e8 and e10. *Circles* mark measurements of SP before start of pumping and at the end (480 min after the start)

pumping wells or artesian springs) there will be positive anomalies. In favourable conditions (e.g. Bogoslovsky and Ogilvy 1972; Parasnis 1986; Ogilvy and others 1989) the positive SP anomaly around a pumping well will be a mirror image of the pressure distribution (drawdown cone) and the change in SP due to pumping will be proportional to the drawdown.

SP signals can be interpreted by the use of analytical (for example, Fitterman 1978; Fournier 1989) or numerical (for example, Sill 1983) models, which provides some means of addressing effects of inhomogeneous ground resistivity. The approach of this study was, however, to interpret the SP data by direct application of the Helmholz-Smoluchovsky equation [Eq. (5)]. This approach has the advantage that it is straightforward and allows for direct calculation of drawdown from SP measurements. Some errors in the calculated drawdown may be expected due to resistivity effects. However, if the resistivity of the unsaturated zone can be assumed to be homogeneous, the change in SP due to pumping is essentially a mirror image of the drawdown. With knowledge of the ζ-potential, fluid electrical conductivity and temperature, and assuming that the "mirror image" model holds, the drawdown can be directly quantified by the use of Eq. (5). The SP measurements at the ten electrode locations thus provide extra drawdown measurements for the hydrogeological analysis.

Interpretation

Interpretation of the SP with time signals is a complex matter. The following basic assumptions have been stated: (1) the measured SP values are stable before the start and at the end of pumping; (2) the change in SP between the end and the start is due to the change in groundwater levels, produced by the pumping; (3) there is no change in groundwater level at the location of the reference electrode, which is unaffected by the pumping. Since the water level at the location of the reference electrode is constant, the change in (mean) head gradient ∇H between each electrode location and the reference is the change in head ΔH at the electrode divided by the distance to the reference. $\Delta H = H_{end} - H_{start} =$ –drawdown; (4) groundwater flow towards the pumping well is horizontal. This condition will in practice be fulfilled at some distance from the pumping well but will not hold at close distances. Under these assumptions the change in SP between the start and end of pumping ($\Delta V = SP_{end} - SP_{start}$) can be used to calculate the drawdown at the end of pumping, at the locations of the electrodes, using the Helmholz-Smoluchovsky equation [Eq. (5)]. The change in electric potential gradient ∇V due to pumping is given by ΔV divided by the distance to the reference electrode. Therefore the quotient $\Delta V/\Delta H$ equals $\nabla V/\nabla H$ (for mean gradients) between each electrode and the reference. The start and end SP values have been extracted from SP-time data as shown in Fig. 8, and the change in SP along with a calculated drawdown value at each electrode is shown in Table 2.

The calculated drawdown values in Table 2 are based on the following: the temperature of the groundwater was 19.5 °C, which gives η=1.02 mPa-s and $\epsilon_r\epsilon_0 = 7.13\times10^{-10}$ F/m. The fluid electrical conductivity σ in the pumping well changed with time during pumping from about 1,132 μS/cm after 18 min (with 36-m drawdown) to 1,550 μS/cm at 480 min (50.4-m drawdown). However, the early σ values are thought to represent σ at shallow depths and are assumed to have the strongest influence on measured SP at the ground surface. Hence σ=1,132 μS/cm is assumed. The ζ-potential was taken to be –33 mV based on the laboratory measurements. [This assumption is somewhat arbitrary, but it is based on borelog data provided by Morton and Love (1998), which may indicate that the rock type is more similar to Q1B or Q2 than Q1A, with an error margin of ±5 or 10 mV.] This gives $C_s' = -2.0$ mV/m, relating change in SP to drawdown.

The increase in SP during the first half and decrease during the second half of the pumping cannot be explained solely by the Helmholz-Smoluchovsky equation; firstly, because then the SP with time curves would have similar shapes to those of drawdown with time at the boreholes (shown in Fig. 7); and secondly, because the change in SP near to its highest value at approximately 280 min is too high to be the product of a reasonable streaming-potential coefficient (C_s') and head gradient (drawdown). The

Table 2
Change in SP and calculated drawdown at each electrode, and measured drawdown in the boreholes. The (apparent) hydraulic conductivities between the pumping well and each point of measurement are also given

Electrode	Change in SP (mV)	Calculated drawdown (m)	Hydraulic conductivity (m/day)
b1	5.7	2.8	0.0367 (min.)
b2	10.5	5.2	0.0404
b3	13	6.5	0.0376
b4	8	4.0	
b5	4.5	2.2	0.0385
e6	12.5	6.2	0.0373
e7	18	9.0	0.0423 (max.)
e8	11.5	5.7	0.0376
e9	23	11.5	0.0414
e10	9.5	4.7	0.0408
Borehole		Measured drawdown (m)	Hydraulic conductivity (m/day)
Bore 1		1.53	0.0347 (min.)
Bore 2		1.02	0.0356
Bore 3		6.71	0.0380 (max.)
Bore 5		0.83	0.0365

analysis using Eq. (5) is hence restricted to the end of pumping, which is not, however, a problem, since the permeability is anyway preferably calculated when the drawdown cone (potentiometric surface) has stabilised at the end of the pumping.

As can be seen in Fig. 7 the drawdown in the wells is not changing significantly with time at the end of pumping and thus steady-state flow can be assumed. Under the assumptions described in 'Groundwater flow towards a production well', the drawdown can be assumed to decrease logarithmically with radial distance from the pumping well and the apparent hydraulic conductivity (K) in the directions where drawdown measurements are available can thus be calculated. Winsor (1998) shows that vertical fractures are frequent on the western side of the Clare Valley. Such fractures may exist along overturned bedding planes and as fractures of "ac" type (see Winsor 1998) orthogonal to the bedding planes. Fractures of "bc" type (orthogonal to bedding and "ac" fractures) improve the connectivity of the system. Watervale has therefore been assumed to be an unconfined aquifer and Eq. (7) has been used to calculate K. The K values based on calculated drawdown at each electrode location are presented in Table 2. The quotient $K_{max}/K_{min}=0.0423/0.0367=1.156$ with maximum hydraulic conductivity in the direction of electrode e7 and minimum for b1. In comparison, similar calculations can be made based on the drawdown measured in the observation wells (see Table 2). According to the boreholes alone $K_{max}/K_{min}=0.0380/0.0347=1.094$. According to both borehole and SP data the aquifer is hence fairly isotropic.

To calculate K, the radius of the pumping well $r_w=103$ mm and the saturated thickness of the aquifer before pumping H_0 are needed. H_0 is assumed to be equal to the depth of the wells minus the drawdown before pumping and hence $H_0=100-7.61=92.39$ m. All the bores are open with no screens and casing only at the top. The drawdown in the pumping well at the end of pumping was 50.39 m and the head loss is assumed to be 2%=1.01 m; hence at radial distance $r=r_w$, the head $H_w=100-50.39+1.01=50.62$ m. The point $(r_w, H_w)=(0.103, 50.62)$ together with the calculated drawdown values at each electrode is used to calculate K between the pumping well at each electrode location. The mixed use of calculated drawdown (based on potential measurements) and measured drawdown in the pumping well is not unrealistic in practical tests, since in any pumping test, including single-well tests, it is always possible to directly measure the drawdown in the pumping well.

Defining the common centre point as described above also makes it possible to calculate the drawdown as a function of radial distance from the pumping well on the basis of each drawdown measurement or calculated drawdown value using Eq. (7). A drawdown curve in each direction can hence be obtained. These curves together form a drawdown cone, which is illustrated in Fig. 9 where contours of equal drawdown around the pumping well have been plotted based on the assumption of logarithmic decrease in drawdown with distance from the well described above. Electrode b4, adjacent to the pumping well, has been omitted in this analysis in order to produce a more realistic plot. There are difficulties in correctly interpreting a streaming-potential measurement taken very close to the pumping well; firstly, because the flow cannot be assumed to be horizontal, and secondly, because the distance to the water table and hence also to the source of electric current, which produces the potential gradient at ground surface, is substantially larger close to the pumping well. However, there could be other reasons to the low value at b4 as well. One possibility is the closeness to the pump, also adjacent to the pumping well, which may have an effect on the electrode.

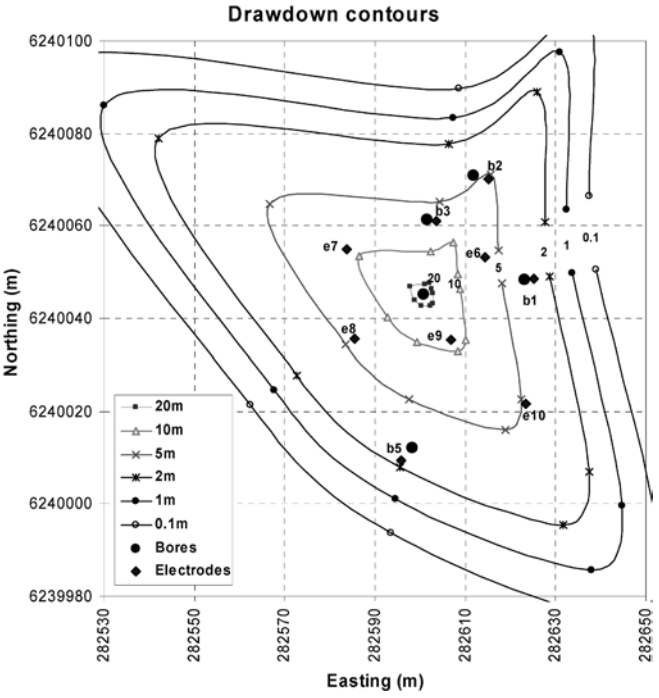

Fig. 9
Spatial drawdown contours based on SP measurements

Figure 9 shows that according to the SP data preferred flow paths towards the pumping well are along the NW–SE axis and from the NNE along a line near bore 2. The drawdown is the lowest towards bore 1, which is consistent with measurements in the bores.

Validation

As a validation of the results, Fig. 10 shows calculated drawdown based on SP measurements together with drawdown measured in the observation wells as a function of radial distance from the pumping well. For comparison, three drawdown curves have been plotted, the maximum (N) and minimum (E) curves based on the borehole data (bore 3 and bore 1), and the maximum curve based on SP data, which is the curve based on the measurement at electrode e7, at 300° relative to geomagnetic north (~NW). As can be seen in Fig. 10, the calculated drawdown at electrode b3 fits very well with the measured drawdown at bore 3 since the value at b3 is on the drawdown curve

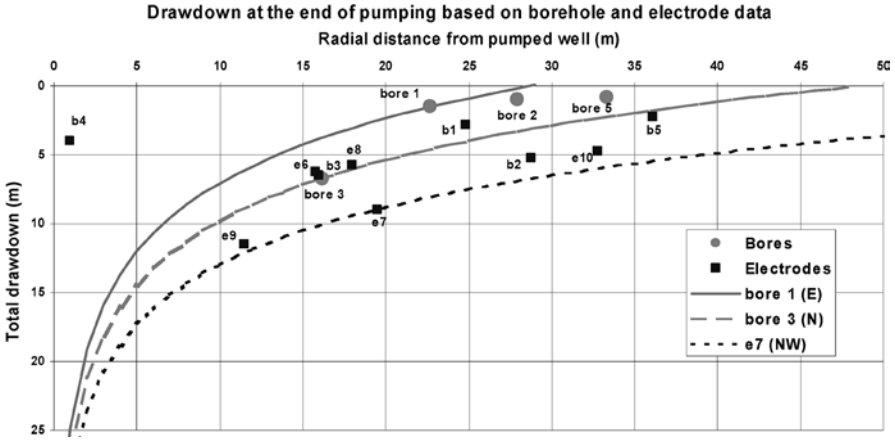

Fig. 10
Drawdown measured in the boreholes (*circles*) and drawdown calculated from SP measurements at the ten electrodes (*squares*). Maximum (N) and minimum (E) theoretical drawdown curves based on borehole data and maximum (NW) curve based on SP data have been plotted for comparison

defined by bore 3. Also the drawdown at b5 falls on this curve possibly indicating symmetry along the north–south axis. The measured drawdown at bore 5 indicates a slightly lower drawdown to the south compared to the north. The measured drawdown at bore 1 is the relatively lowest since it indicates the lowest hydraulic conductivity and produces the lowest theoretical drawdown curve. The calculated drawdown at the adjacent electrode b1 is also the (relatively) lowest of the SP-based values, which is consistent with piezometer measurements. The drawdown according to b2 is lower than the measured value at bore 2. Electrodes e7, e9, e10 and b2 show higher drawdowns than what is measured in the bores. e7, e9, and e10 all lie on the NW–SE axis through the pumping well and are roughly on the same "drawdown with distance curve", which may indicate fractures along this axis. Electrode b4 adjacent to the pumping well shows an unreasonably low drawdown. On the whole, drawdown based on SP measurements is reasonable. It decreases with radial distance in a manner consistent with logarithmic decrease predicted by theory. On average the SP-based drawdown is somewhat higher than what was measured in the bores. This could be because the bores constitute only measurements along the N–S axis and one to the E but none along the NW–SE axis. It is also possible that the increasing–decreasing trend seen in Fig. 8 had not completely settled by the end of pumping, thus making all SP values slightly too high. The drawdown in the N–S direction according to borehole measurements is not contradicted by the SP, but the SP shows a different direction of maximum drawdown, the NW–SE (see Fig. 9), which is not tested by the observation wells.

Noise and drift considerations

By measuring the change in SP due to pumping, the unwanted noise contribution from all time-constant SP sources can be cancelled out. This works provided that the SP signal originates from independent SP sources that can be superpositioned unambiguously to produce the total value. The use of change in SP rather than "static" SP is hence a way of greatly reducing errors.

The most important source of error in SP surveys is probably electrode drift due to spatial differences and changes with time in soil moisture and temperature around the electrodes (Schiavone and Quarto 1984; Wanfang and others 1999). To minimise drift the electrodes should be carefully prepared and field procedures meticulously done. By measuring change in SP due to pumping, errors caused by spatial differences can be minimised. Furthermore, the electrodes should be buried well in advance of the pumping (preferably the day before) to ensure that a stable signal before the start of pumping is obtained. The electrodes should ideally be placed where the soil conditions do not change significantly with time. Watering of the electrodes should be avoided.

Changes in the Earth's external magnetic field produce induced electric currents in the ground and thus affect the electric field and measured SP. The longer the distance over which a potential difference is measured (the larger the dipole) the higher is the magnetically induced noise. This type of noise can hence be kept low by measuring potential differences over relatively short distances (as in this study). The change in electric potential is dependent on the frequency of the magnetic field variation and the resistivity of the ground. To obtain the exact response in potential seems not to be possible without knowledge of the resistivity down to a depth of tens of kilometres. Nevertheless magnetic data for the time periods of the field study were obtained from the Australian Geological Survey Organisation, Canberra. Data were compared with the measured SP and a simple analysis showed that variation in the Earth's magnetic field affects SP and induces short-term variation in the measured signal, but the longer SP trends are not correlated to magnetic variation.

Discussion and conclusion

Results from the field study indicate that SP signals generated during pumping tests are complex and the processes controlling them are not fully understood. The signals produced at early stages of pumping are not proportional to ∇H as predicted by the Helmholz-Smoluchovsky equation. However, after several hours of pumping and as the change in drawdown with time becomes insignificantly small, the SP signal stabilises to a constant value. Laboratory experiments show that if water has been

standing in the pores of a rock sample for some time and then a pressure gradient is applied making the water start flowing, it normally takes some time before the SP signal stabilises and a linear relationship between streaming potential and pressure gradient can be observed. Both field and laboratory experiments therefore indicate that some equilibrium processes at the rock–water interface may be of importance as changes in pressure gradients and flow velocities take place. To improve our understanding of SP generated during pumping tests this may be worth investigating in more detail.

SP has various different sources and it is therefore often hard to isolate the signal generated by a specific process. However, the pumping of water from a well makes it possible to study the change in SP solely due to pumping. This procedure eliminates the errors otherwise induced by any time-constant other SP sources present. The relatively simple and straightforward relationship between SP and drawdown given by Eq. (5) proved satisfactory for determining drawdown in the test area at Watervale Oval. Here the calculated drawdown was consistent with the drawdown measured in observation wells. The results indicate that such "simple" calculations may determine drawdown accurately, provided that (1) the SP signals are correctly interpreted, (2) the SP-generating processes are in equilibrium and (3) the signals are isolated from noise (other SP sources). To determine the drawdown this way it is sufficient to measure the SP prior to pumping and then again once steady-state conditions have been reached. Continuous SP measurements in this study have, however, provided useful information about pitfalls and limitations of the method.

To quantify the drawdown based on SP measurements, knowledge of the fluid electrical conductivity and the ζ-potential is essential. The former can easily be measured in the field during pumping whereas the latter may be determined in the laboratory, as it is not generally possible to find the ζ-potential for a given rock type in the literature. The ζ-potentials for three common rock types of the Clare Valley were determined and it was shown that ζ-potentials vary considerably over short distances within this area. The results in this paper indicate that the presence of clay in the rock may have a negative influence on the magnitude of the ζ-potential and that a higher quartz content may have a positive influence.

The main limitations of using SP measurements during pumping tests to determine drawdown have been found to arise from: (1) electrode drift; (2) instability in the streaming potential generating processes, which seems to subsist until equilibrium is established at the rock–water interface; and (3) other SP sources that are not constant with time but are affected by pumping.

Long pumping tests (12–24 h or more) are recommended to allow time for the SP-generating processes to stabilise. Long pumping tests also have the advantage that when the drawdown is in steady state, permeability calculations are straightforward (Thiem's equation can be used). Other SP sources that are affected by pumping are more difficult to address. It seems, however, that if the SP signal is sufficiently large, these effects will be comparatively small. To add certainty to the drawdown calculations it is also recommended that at least two SP measurements be taken along the same transact at different radial distances from the pumping well. This means that three points (the measured drawdown in the pumping well and the calculated drawdown at the two points of SP measurement) are available to fit a logarithmic drawdown curve according to Thiem's equation, which allows validation of consistency of results.

It can be concluded that the success in determining drawdown along with permeability and possible preferred flow paths at Watervale Oval shows that SP methods have potential to provide excellent information about aquifer parameters such as permeability and anisotropy. SP methods in conjunction with pumping tests allow drawdown measurements to be taken without the restriction to existing piezometers and hence have the potential to greatly enhance the accuracy of such hydrogeological investigations, especially in the anisotropic environments of fractured rock aquifers.

Acknowledgements Pumping tests undertaken by CSIRO/Department for Water Resources, South Australia, and by Australian Water Environments made this project possible. The authors would like to thank Andrew Love and Glenn Harrington at CSIRO/Department for Water Resources, South Australia, and Andrew Telfer at Australian Water Environments for providing drawdown measurements in observation wells, fluid electrical conductivity, pH and temperature measurements, which were of excellent value to this paper. The authors would like to thank Damien Skinner, Ben Hopkins, Amelie Roy and Mathieu Brochu for help in the field and John Stanley for assistance in the laboratory. The authors are grateful for funding from the University of Adelaide's "Small Research Grants Scheme 2001".

References

Ahmad MU (1964) A laboratory study of streaming potentials. Geophys Prospect 12:49–64

Bear J (1979) Hydraulics of groundwater. McGraw-Hill, Keterpress, Jerusalem

Bogoslovsky VV, Ogilvy AA (1972) Deformations of natural electric fields near drainage structures. Geophys Prospect 21:716–723

Corwin RF, Hoover DB (1979) The self-potential method in geothermal exploration. Geophysics 44:226–245

Fetter CW (1994) Applied hydrogeology, 3rd edn. Prentice-Hall, Englewood Cliffs

Fitterman DV (1978) Electrokinetic and magnetic anomalies associated with dilatant regions in a layered earth. J Geophys Res 83:5923–5928

Fournier C (1989) Spontaneous potentials and resistivity surveys applied to hydrogeology in a volcanic area: case history of the Chaîne des Puys (Puy-de-Dôme), France. Geophys Prospect 37:647–668

Heinson G, Segawa J (1997) Electrokinetic signature of the Nankai Trough accretionary complex: preliminary modelling for the Kaiko-Tokai program. Phys Earth Planet Int 99: 33–53

Ishido T, Mizutani H (1981) Experimental and theoretical basis of electrokinetic phenomena in rock–water systems and its applications to geophysics. J Geophys Res 86:1763–1775
Ishido T, Pritchett JW (1999) Numerical simulation of electrokinetic potentials associated with subsurface fluid flow. J Geophys Res 104:15247–15259
Ishido T, Mitzutani H, Baba K (1983) Streaming potential observations, using geothermal wells and in situ electrokinetic coupling coefficients under high temperature. Tectonophysics 91:89–104
Jansen J, Zorich T (1995) Spontaneous potential surveys around pumping wells. In: Proc Symp of Applied Geophysics to Environmental and Engineering Problems (SAGEEP), pp 865–869
Jouniaux L, Pozzi J-P (1995a) Permeability dependence of streaming potential in rocks for various fluid conductivities. Geophys Res Lett 22:485–488
Jouniaux L, Pozzi J-P (1995b) Streaming potential and permeability of saturated sandstones under triaxial stress: consequences for electrotelluric anomalies prior to earthquakes. J Geophys Res 100:10197–10209
Kaye GWC, Laby TH (1986) Tables of physical and chemical constants, 15th edn. Longman, London
Lorne B, Perrier F, Avouac J-P (1999) Streaming potential measurements. 1. Properties of the electrical double layer from crushed rock samples. J Geophys Res 104:17857–17877
Love A, Cook P (1998) The Clare Valley – a fractured rock aquifer. Information Sheet January 1998. Department of Primary Industries and Resources South Australia (PIRSA), Adelaide
Love A, Cook P (1999) The importance of fractured rock aquifers. Report Book 99/23 Department of Primary Industries and Resources South Australia (PIRSA), Adelaide
Morgan FD, Williams ER, Madden TR (1989) Streaming potential properties of westerly granite with applications. J Geophys Res 94:12449–12461
Morton D, Love A (1998) Clare Valley groundwater resources, progress report 2, drilling phase II. Report Book 98/14. Department of Primary Industries and Resources South Australia (PIRSA), Adelaide
Morton D, Love AJ, Clarke D, Martin R, Cook PG, McEvan K (1998) Clare Valley groundwater resources, progress report 1, hydrogeology, drilling and groundwater monitoring. Report Book 98/15. Department of Primary Industries and Resources South Australia (PIRSA), Adelaide
Ogilvy AA, Ostrovskij EJ, Ruderman EN (1989) Electrical surveys using the method of the natural electric field; new investigations. In: Merkler GP and others (eds) Detection of subsurface flow-phenomena. Lecture notes in earth sciences, 27. Springer, Berlin Heidelberg New York, pp 401–466
Overbeek JThG (1952) IV. Electrochemistry of the double layer and V. Electrokinetic phenomena. In: Kruyt HR (ed) Colloid science, vol I, irreversible systems. Elsevier, Amsterdam, pp 115–243
Parasnis DS (1986) Principles of applied geophysics, 4th edn. Chapman and Hall, London
Revil A, Pezard PA, Glover PW (1999a) Streaming potential in porous media 1. Theory of the zeta potential. J Geophys Res 104:20021–20031
Revil A, Schwaeger H, Cathles LM, Manhardt PD (1999b) Streaming potential in porous media, 2. Theory and application to geothermal systems. J Geophys Res 104:20033–20048
Schiavone D, Quarto R (1984) Self-potential prospecting in the study of water movements. Geoexploration 22:47–58
Sill RW (1983) Self-potential modeling from primary flows. Geophysics 48:76–86
Truesdail SE, Westermann-Clark GB, Shah DO (1998) Apparatus for streaming potential measurements on granular filter media. J Environ Eng 124:1228–1232
Wanfang Z, Beck BF, Stephenson JB (1999) Investigation of groundwater flow in karst areas using component separation of natural potential measurements. Environ Geol 37(1–2):19–25
Winsor CN (1995) Proc Conf Structural Geology and Tectonics Specialist Group (SGTSG), Clare Valley, 25–29 Sept, Abstract, pp 177–178
Winsor CN (1998) Clare Valley – a fractured rock aquifer: review of surface discontinuities. Internal Report. Department of Primary Industries and Resources South Australia (PIRSA), Adelaide